Structures 47 (2023) 2050–2065

Contents lists available at ScienceDirect

Structures

journal homepage: www.elsevier.com/locate/structures

Assessment of the effects of non-structural components on the seismic reliability of structures via a block diagram method

Vahid Mohsenian [a,*], Nima Gharaei-Moghaddam [b], Stefano Mariani [c], Iman Hajirasouliha [d]

[a] Department of Civil Engineering, University of Science and Culture, Iran
[b] Department of Civil Engineering, School of Engineering, Ferdowsi University of Mashhad, Iran
[c] Department of Civil and Environmental Engineering, Politecnico di Milano, Italy
[d] Department of Civil and Structural Engineering, The University of Sheffield, UK

ARTICLE INFO

Keywords:
Non-structural components
Seismic reliability analysis
Block diagrams
Series components

ABSTRACT

Under a specific ground motion excitation, even if structural components all satisfy a target performance level, the serviceability of the structure might get affected by the performance of non-structural components. Although the overall performance of a structure is affected by the performance of both structural and non-structural components, seismic reliability and fragility analyses usually only focus on the structural elements and their load-carrying capacity. The present study aims to assess the influence of the acceleration-sensitive non-structural components on the seismic reliability of the entire structure. The distinguishing feature of the proposed approach is the adoption of reliability block diagrams for the analysis of each structure, allowing for different combinations of damage for structural and non-structural components. Results are shown for 5-, 10- and 15-story buildings, to demonstrate the significant effects of non-structural components on their overall seismic reliability. Such effects prove to be more evident for the lower damage levels, and the higher seismic intensities. It is shown that non-structural components can lead to a reduction of the overall seismic reliability ranging from 22% to 100%, for situations related to the life safety and collapse prevention performance levels, under the effects of the design basis and maximum considered earthquakes, respectively.

1. Introduction

The existence of a wide variety of non-structural components in residential buildings and infrastructures, featuring varying importance levels, actually represents a challenge to set an appropriate uniform strategy for the analysis and design under the effects of uncertain (future) ground motions. In the case of a design basis earthquake, extensive damage to the non-structural components can interrupt the serviceability of the structures, as shown by the actual and extreme situation depicted in Fig. 1. It is also proved that the failures of non-structural components make up the majority of earthquake damage [1]. Therefore, the performance level of the whole structural system has to be defined as a proper combination of the performance levels of its structural and non-structural components [2].

As non-structural components are assumed not to play a dominant role in carrying lateral loads, in the design of structural systems these elements are usually not considered under seismic actions. However, the results of recent earthquakes and extensive damage developed in the non-structural components proved the importance of considering the performance of these components in the process of overall seismic performance evaluation of buildings and infrastructures [3]. Accordingly, various studies have been performed on the behavior and design of different types of non-structural components.

Most of the previous investigations on non-structural components can be categorized into two general groups. The first category includes experimental studies aimed at investigating the seismic performance of different forms of non-structural components. For instance, Zhou *et al.* [4] performed shaking table tests to assess the seismic performance of displacement-sensitive non-structural components. They proposed a multi-directional decoupling iteration control method to accurately reproduce floor response spectra. Jenkins *et al.* [5] performed full-scale tests on a two-story braced frame structure to study the seismic performance of integrated ceiling-piping-partition systems and developed fragility functions for cold-formed steel-framed partitions. Based on their attained results, the accuracy of the amplification factors recommended by the code for flexible partition walls was verified. Another

* Corresponding author.
E-mail addresses: v.mohsenian@usc.ac.ir (V. Mohsenian), i.hajirasouliha@sheffield.ac.uk (I. Hajirasouliha).

https://doi.org/10.1016/j.istruc.2022.12.024
Received 15 July 2022; Received in revised form 8 November 2022; Accepted 9 December 2022

Fig. 1. Extensive damage to the non-structural components of a building after the Kermanshah 2017 earthquake, Iran (picture taken by one of the authors).

experimental study was conducted by Hou *et al.* [6], by performing shake table tests on full-scale steel frame structures equipped with tension-only braces. In their study, the authors considered the influence of the stiffness of non-structural components on their horizontal force demand. Based on these results, Hou *et al.* evaluated the adequacy of the existing design models and also proposed improved design relations. Raffaele *et al.* [7] also conducted an extensive experimental study to assess the seismic performance of lightweight steel drywall non-structural components.

In the second category of the studies on non-structural components, usually analytical and/or numerical approaches have been developed to assess their seismic demand and accordingly modify the design code recommendations. For example, Anajafi and Medina [8] evaluated the accuracy of the equation proposed by ASCE 7–16 to estimate it, using data from instrumented buildings as well as numerical models, getting to the conclusion that the mentioned relations are not reliable. In other similar studies, Magliulo *et al.* [9] and Fathali and Lizundia [10] assessed the adequacy of Eurocode 8 and ASCE 7–05 provisions to compute the seismic demand; these studies showed that such provisions may not provide satisfactory predictions. Mohsenian *et al.* [11] also showed that the relations proposed by ASCE7-16 and NIST regarding the acceleration demand of acceleration-sensitive non-structural components provide inaccurate estimations; using a multi-level approach, a relation for estimating the maximum absolute acceleration distribution along the height of structures was then proposed. Salari *et al.* [12] also investigated the demands of acceleration-sensitive non-structural components in special concentrically braced frames and moment-resisting frames. In this study, the authors investigated the effect of the ratio of non-structural components period to structural period, their damping ratio, and vertical location on their demands.

In an attempt to determine the seismic response of acceleration-sensitive non-structural components, Lima and Martinelli [13] performed a parametric analysis to capture the key features of the dynamic response of a coupled two-degree-of-freedom system, representative of the main structure and the non-structural components. Villaverde [14] also proposed a simple method, based on the analysis of linear secondary systems mounted on a linear primary structure, to estimate the seismic response of non-structural components. Wang *et al.* [15] recently published a state-of-the-art review on this topic.

The critical review of the literature reported here above shows that, despite the extensive investigations in this area, the number of studies about the influence of non-structural components on the reliability of the whole structural system is limited. In one of the available studies, Sullivan [16] evaluated the role of non-structural components on the post-earthquake performance of structures, allowing for the effect of the design and detailing of non-structural elements on the reparability of buildings. In another study, Perrone *et al.* [17] developed a methodology for performance evaluation of non-structural components based on performance-based design philosophy. The proposed framework can be considered as an equivalent of the suggested methodology by FEMA P695 for the force-based design of seismic force-resisting systems. In a study on the seismic risk analysis of the Vancouver metropolitan region performed by Mahsuli and Haukaas [18], it was also shown that non-structural components contribute more to the losses than structural ones.

A research gap is especially evident in the probabilistic studies to develop seismic fragility curves for different structural systems. In this case, most of the performed studies utilized empirical data for the development of fragility curves. In one of the studies in this field, Kuo *et al.* [19] provided a process to derive the fragilities of non-structural elements using a damage survey. In another study, Cremen and Baker [20] proposed a method to modify the fragility functions and loss predictions of non-structural components according to FEMA P-58. For this purpose, they suggested using the maximum likelihood approach to fit the fragility functions to the underlying empirical data, which mitigates the convergence problems during the fitting process.

As discussed above, a reliability analysis of structures by considering different combinations of damage levels for structural and non-structural components is rather limited. The present study thus represents an important step to address some of the challenging issues in this area. The main contributions of this work can be listed as follows:

i. The role of the non-structural components in the seismic reliability of structures is assessed, and general rules to guide the selection of the performance levels for structural and non-structural components under the design basis and the maximum considered earthquakes are provided.
ii. A novel modelling approach is proposed to estimate the reliability of structures, by considering the effects of both structural and non-structural components using the block diagrams concept.
iii. A new methodology based on performance areas is introduced, to allow for the values of the response parameters in continuous ranges and move beyond what is linked to the predefined limit states.

2. Methodology

In this study, the seismic reliability analyses of multi-storey structures have been performed by adopting four different approaches, namely the standard approach, story-wise approach, block diagram approach, and performance areas approach. All these methods require providing a set of statistical data from the seismic response of structures in specific seismic hazard levels. For this purpose, it is required to first analyze the considered structure subjected to a series of accelerograms (scaled to the desired intensity).

In the standard reliability analysis method, the maximum responses in the structure under each ground motion record are considered irrespective of their locations. Subsequently, for each structural and non-structural component, the reliability of not experiencing different damage levels is calculated separately. Although this approach is efficient, it cannot take into account the effect of damage location.

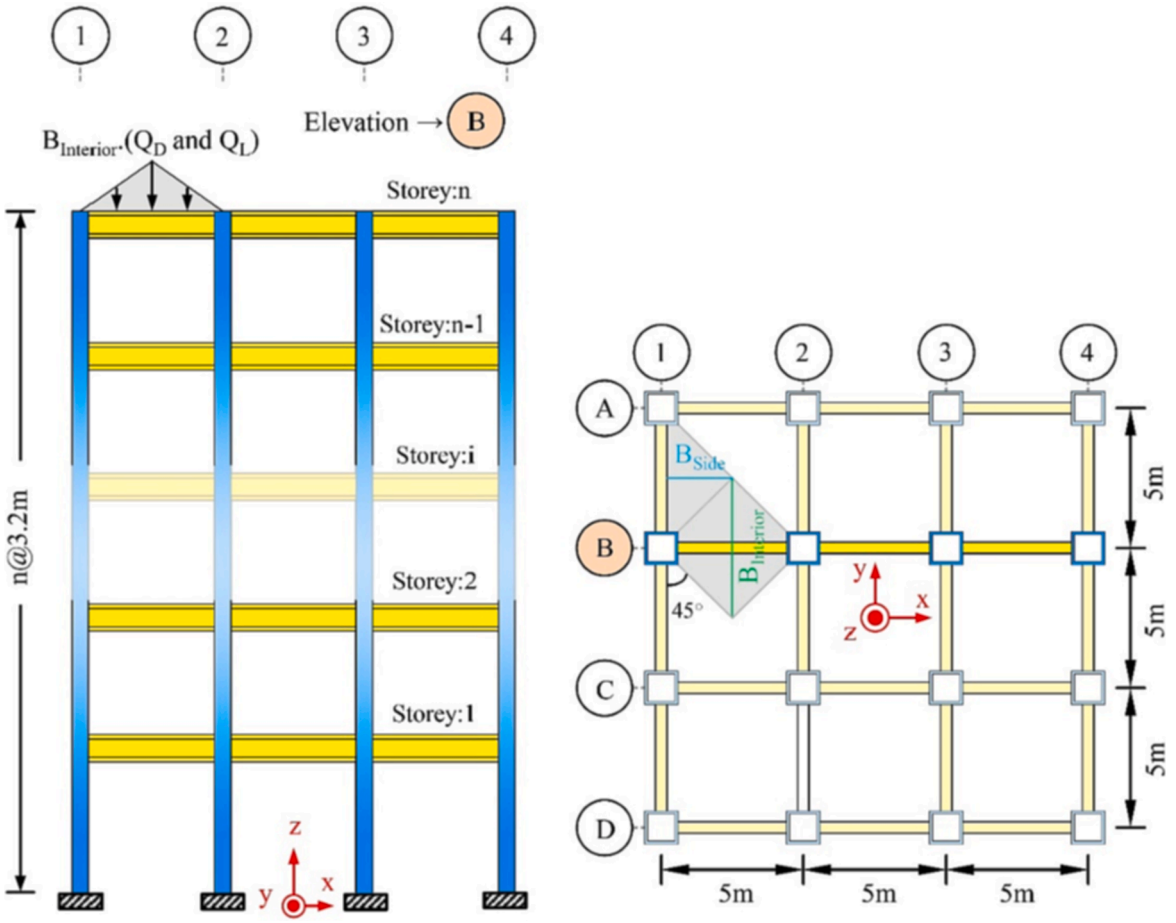

Fig. 2. Schematic side elevation and plan of the structures, loading conditions and geometrical properties.

Moreover, it is not possible to provide an overall reliability estimation for the entire structural system considering the effects of both structural and non-structural components.

In the second utilized technique, called story-wise approach, the reliability of each story is calculated separately, and then the minimum computed reliability is considered for the entire structure. In contrast with the standard method, in this approach the critical damage locations at the height of the structure can be detected easily. However, this methodology also fails to combine the influences of both structural and non-structural components in the reliability analysis process.

In the block diagram approach, the structure is modelled using a set of parallel and series components, and the reliability is calculated based on the combined reliability of structural and non-structural components. The story-wise method is a prerequisite for the block diagram methodology, and accordingly, the critical damage locations are also reflected in the block diagram method. In addition, this proposed technique provides the possibility to perform reliability analysis considering different combinations of damages for structural and non-structural components. Thus, the block diagram approach can address some of the limitations of the other available approaches as discussed above.

Under a given seismic intensity, the reliability analysis is performed considering certain damage levels for structural and non-structural components. However, since structural damage is a continuous variable, using specific predefined limits may not be very reasonable. To address this issue, it is proposed to use performance areas instead of limit states.

The above described reliability analysis methods have been performed on a set of selected structures (Section 3). It should be noted that the proposed methodologies are independent of the properties of the studied structures (e.g. geometry, height, loading details, lateral load-resisting system, type of non-structural components) and also the considered seismic excitations. Section 4 presents the details of each analysis mythology and its implementation steps as well as the analysis results. Finally, the concluding remarks are given in Section 5.

3. Properties of the models and details of the nonlinear modeling approach

In this study, the three multi-story moment-resisting steel frame structures, already considered in ref. [11], have been analyzed. To investigate the effects of the structural height on the response to the ground motion, the frames feature 5, 10, and 15 stories. The details related to the building plan, the reference frame, and the design loads are reported in Fig. 2. The sections of the considered frame structures and relevant coding for the beams and columns are also illustrated in Fig. 3. The cross-sections of the structural members are denoted according to the additional details provided in Table 1, where B and C respectively denote beam and column elements. The story height and the span length have been set to 3.2 m and 5 m, respectively, while a concrete slab was used for the roof system. The selected frames are symmetric about the $x-z$ and $y-z$ planes, and represent typical building structures in Iran.

The structural components have been assumed to be made of A36 steel, with a yield stress of 250 MPa and a Poisson's ratio of 0.26 [21]. The structural systems have been designed according to AISC360-210 [22], using the ETBAS software [23] and assuming a medium importance and very high seismicity of the site (characterized by a PGA = 0.35 g, where g is the gravitational acceleration). According to ASCE7-10 [24], the site soil has been assumed of type C with a shear wave velocity between 375 and 750 m/s. Dead Q_D and live Q_L loads of 6.3 and 2 kN/m^2

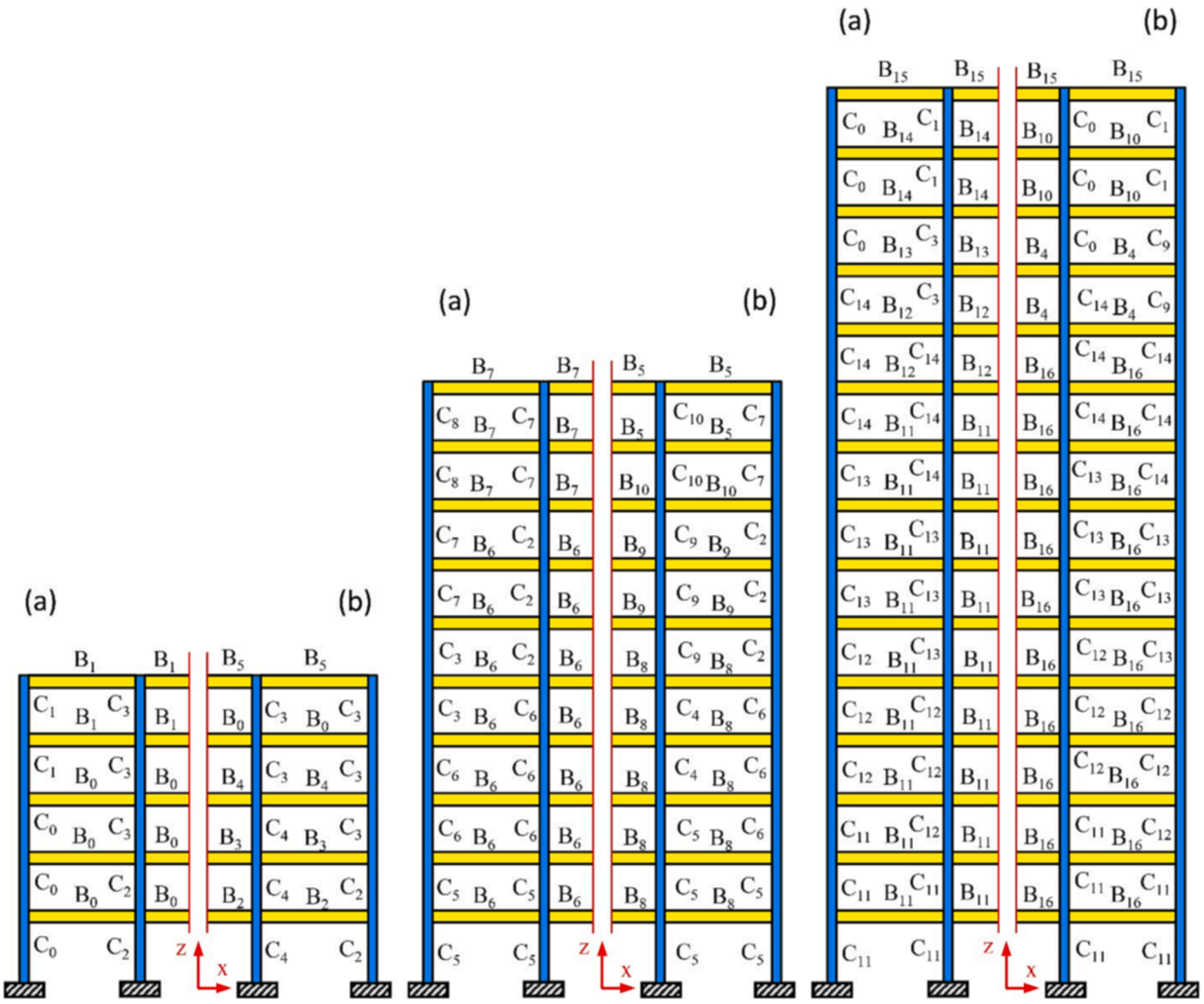

Fig. 3. Vertical sections of the three considered frame structures, and relevant coding for the beams and columns: (a)-side frames (denoted as 1, 4, A, and D in Fig. 1), (b)-middle frames (denoted as 2, 3, B, and C in Fig. 1). Notice that building symmetries have been accounted for in these schemes.

Table 1
Section properties of beams and columns reported in Fig. 2 (dimensions are in mm).

Columns		Beams	
ID	Section: (width × thikness)	ID	Section: (width × thikness)
C_0	Box (270 × 15)	B_0	Web (270 × 10)-Flanges (150 × 20)
C_1	Box (240 × 15)	B_1	Web (200 × 10)- Flanges (150 × 15)
C_2	Box (350 × 15)	B_2	Web (350 × 10)- Flanges (180 × 20)
C_3	Box (300 × 15)	B_3	Web (350 × 10)- Flanges (200 × 20)
C_4	Box (400 × 20)	B_4	Web (300 × 10)- Flanges (200 × 20)
C_5	Box (500 × 20)	B_5	Web (240 × 10)- Flanges (150 × 20)
C_6	Box (400 × 15)	B_6	Web (300 × 10)- Flanges (150 × 20)
C_7	Box (250 × 15)	B_7	Web (300 × 10)- Flanges (150 × 15)
C_8	Box (200 × 15)	B_8	Web (350 × 10)- Flanges (250 × 25)
C_9	Box (300 × 20)	B_9	Web (350 × 10)- Flanges (200 × 25)
C_{10}	Box (200 × 20)	B_{10}	Web (270 × 10)- Flanges (180 × 20)
C_{11}	Box (650 × 25)	B_{11}	Web (350 × 10)- Flanges (300 × 20)
C_{12}	Box (550 × 25)	B_{12}	Web (320 × 10)- Flanges (250 × 20)
C_{13}	Box (450 × 20)	B_{13}	Web (270 × 10)- Flanges (200 × 10)
C_{14}	Box (350 × 20)	B_{14}	Web (240 × 10)- Flanges (140 × 20)
–	–	B_{15}	Web (200 × 10)- Flanges (150 × 20)
–	–	B_{16}	Web (320 × 10)- Flanges (220 × 20)

have been applied to all the stories. As sketched in Fig. 2, the gravitational loads have been applied with a linear variation along the beam elements, allowing for the widths B_{side}, related to the side beams, and $B_{interior}$, related instead to the interior beams.

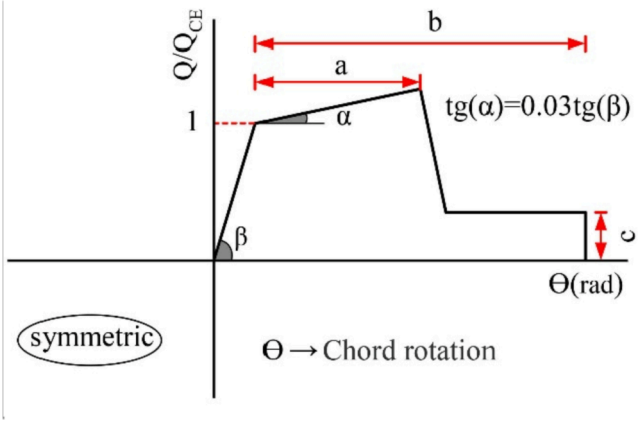

Fig. 4. Generalized force–displacement curve for the steel members.

The PERFORM-3D software [25] has been used to model the structures in their nonlinear range of behavior. In the analyses, lateral and gravitational loadings have been combined according to the following equation, see [26] and Fig. 2:

$$Q_G = Q_D + 0.25Q_L \quad (1)$$

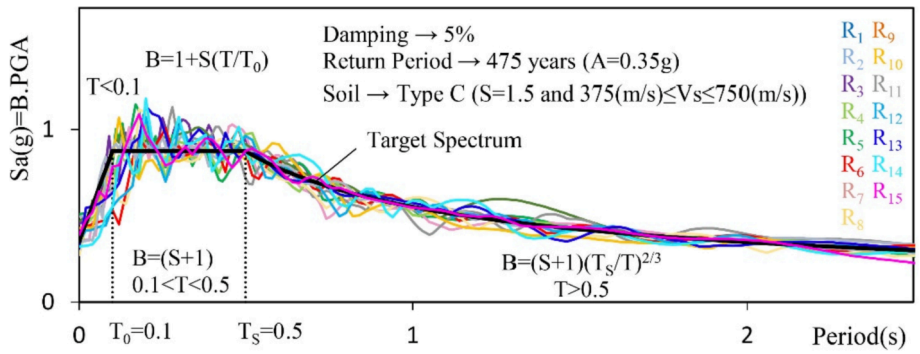

Fig. 5. Comparison of the artificial accelerograms with the demand spectrum of the site.

Table 2
Original ground motion records used to obtain the artificial accelerograms.

Records	Earthquake & Year	Station	R[a](km)	Component	Mw	PGA(g)
R_1	Cape Mendocino (US), 1992	Eureka – Myrtle & West	41.97	90	7.1	0.18
R_2	Cape Mendocino (US), 1992	Loleta Fire Station	25.91	270	7.1	0.26
R_3	Cape Mendocino (US), 1992	Fortuna – Fortuna Blvd	19.95	0	7.1	0.12
R_4	Chi-Chi (Taiwan), 1999	TCU042	26.31	E	7.6	0.25
R_5	Chi-Chi (Taiwan), 1999	TCU070	19.00	E	7.6	0.25
R_6	Chi-Chi (Taiwan), 1999	TCU106	15.00	E	7.6	0.16
R_7	Darfield (New Zealand), 2010	Heathcote Valley Primary School	24.50	E	7.0	0.63
R_8	Iwate (Japan), 2008	Yuzawa Town	25.56	NS	6.9	0.24
R_9	Iwate (Japan), 2008	Tamati Ono	28.90	NS	6.9	0.28
R_{10}	Kern County (US), 1952	Taft Lincoln School	38.42	111	7.4	0.18
R_{11}	Kocaeli (Turkey), 1999	Iznik	30.73	90	7.5	0.13
R_{12}	Landers (US), 1992	Barstow	34.86	90	7.4	0.14
R_{13}	Montenegro(Yugoslavia), 1979	Herce Novi - O.S.D. Paviviv	23.59	90	7.1	0.26
R_{14}	Northridge (US), 1994	Hollywood – Willoughby Ave	23.07	180	6.7	0.24
R_{15}	Northridge (US), 1994	Big Tujunga, Angeles Nat F	19.74	352	6.7	0.25

[a] Closest distance to fault rupture

A generalized force–displacement relation has been adopted to model the behavior of beams and columns, as illustrated in Fig. 4. In this figure, Q and θ are the flexural capacity and the chord rotation of the element, respectively. Parameters a, b and c in the response curve are taken from the modeling and acceptance criteria for the nonlinear analysis of steel structural components reported in [26]. The maximum expected strength Q_{CE} of the structural members is then given by:

$$Q_{CE} = ZF_{ye} \tag{2}$$

$$Q_{CE} = ZF_{ye}\left(1 - \frac{|P|}{2P_{ye}}\right) \quad for \quad \left(\frac{|P|}{P_{ye}} < 0.2\right) \tag{3}$$

$$Q_{CE} = \frac{9}{8}ZF_{ye}\left(1 - \frac{|P|}{P_{ye}}\right) \quad for \quad \left(\frac{|P|}{P_{ye}} \geqslant 0.2\right) \tag{4}$$

Here, Z is the plastic modulus of the considered cross-section of the member; F_{ye} is the expected yield strength of the material; P is the axial force in the member induced by the gravity load at the beginning of the dynamic analysis; P_{ye} is the expected axial force in the member at yielding given by $P_{ye} = AF_{ye}$, A being the area of its cross-section.

Beams and columns have been all modeled as linear elements, with concentrated hinges of rotation type located at their ends only. In the study, the beam-to-column connections and column bases are modelled as rigid. The dynamic interaction between structural and non-structural components has been investigated extensively and based on the reported results, this effect can be neglected provided that the mass ratio of non-structural to structural components is less than 1 % [27–29]. In this circumstance, it is generally acceptable not to include the acceleration-sensitive non-structural components in the model and perform decoupled dynamic analysis to assess their demands. In the present study, it has been assumed that non-structural components are light enough to satisfy this condition.

4. Seismic reliability analysis

The seismic reliability analysis is now described, to deal with the frequent, design basis, and maximum considered earthquakes with return periods of 10 years, 475 years, and 2475 years, respectively. To this aim, time histories related to the dynamic structural responses have been collected; fifteen ground motion records for each hazard level have been used, in accordance with former works that showed how this number proves enough to reduce the inherent uncertainties in the analysis. To attain consistency with the design spectrum (of Iran's seismic design code) [30], artificial records have been adopted as reported, e.g. in Fig. 5 for the dataset referring to the design basis return period. Accelerograms were obtained by means of the wavelet transform method proposed in [31], and by modifying the original records listed in Table 2. These records are categorized as far-field and are taken from the PEER database for the site soil type c corresponding to the shear wave velocity between 375 and 750 m/s [32]. It should be mentioned that these records have been used in previous studies for performing incremental dynamic analysis and production of artificial accelerograms (considering different spectrums and tolerances) [33,34].

4.1. Seismic reliability analysis by means of standard approach

Fragility curves for the structural and non-structural components (acceleration-sensitive) have been obtained as follows:

i. The artificial accelerograms have been scaled to the peak ground acceleration for the target hazard level, and then used to excite the structures. The target earthquakes have been obtained by

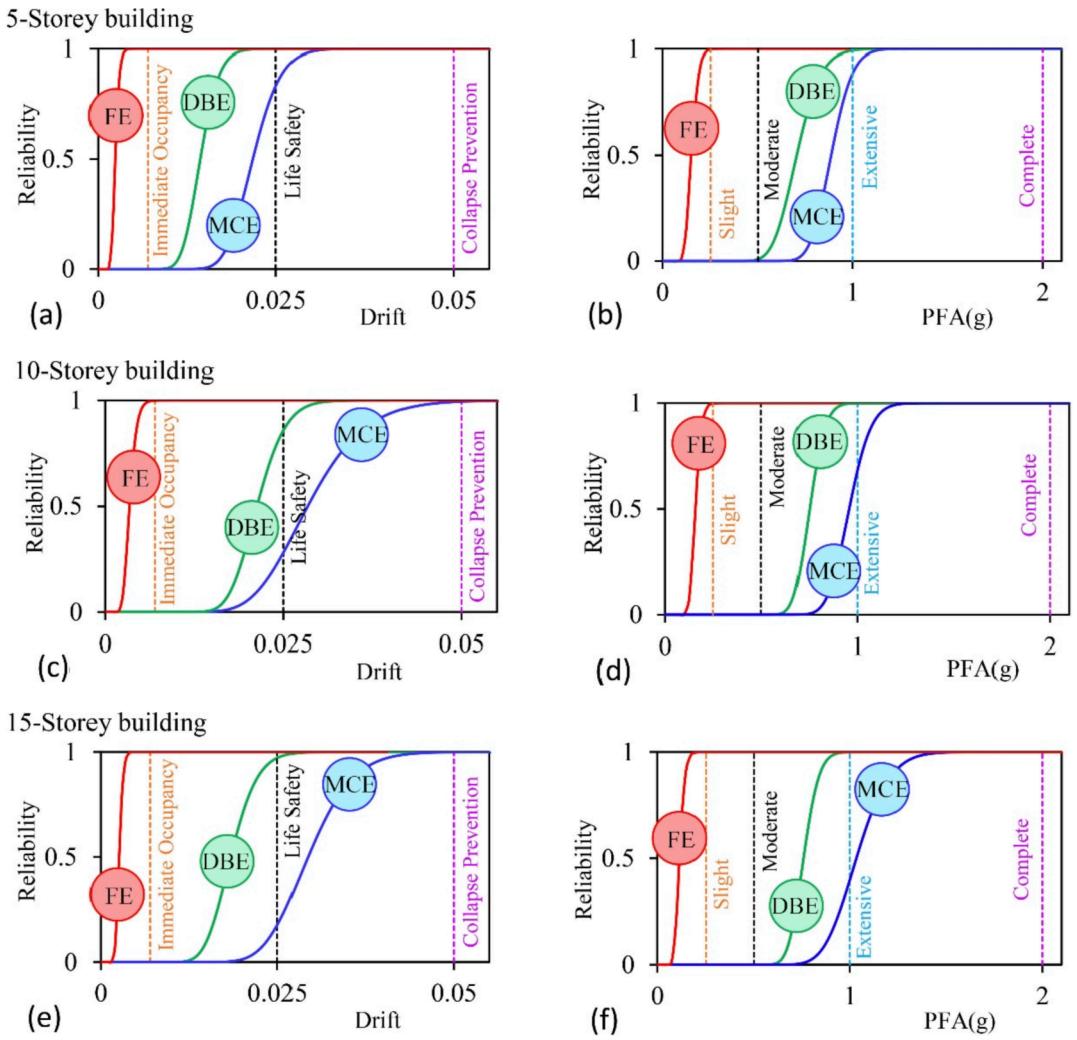

Fig. 6. Reliability curves obtained with the standard approach for the structural (a, c and e) and non-structural components (b, d and f), under different hazard levels and for limit states corresponding to different damage levels.

modifying the Design Basis Earthquake (DBE), through a factor amounting to 0.2 and 1.5 for the Frequent Earthquake (FE) and the Maximum Considered Earthquake (MCE), respectively featuring $PGA_{FE} = 0.07$ g, $PGA_{DBE} = 0.35$ g, and $PGA_{MCE} = 0.52$ g.

ii. The structural response corresponding to the selected damage measure (DM) has been obtained in terms of the maximum inter-story drift for the structural components, and the maximum horizontal story acceleration for the non-structural components. Hereafter, this latter parameter is termed Peak Floor Acceleration (PFA).

iii. Assuming a lognormal distribution for the data collected in step ii), the relevant mean value and standard deviation for each hazard level have been determined.

iv. By considering a target response corresponding to a given performance level, the probability not exceeding the predefined performance level, *R*, has been computed. This value states that for the selected earthquake intensity level, there exists a probability *R* that the structural response does not exceed the corresponding performance level. By varying the value of the structural response for the considered performance level, the reliability curves have been built for all the hazard levels, see also [35,36].

Using the proposed procedure, the reliability curves for the studied structures have been obtained as depicted in Fig. 6.

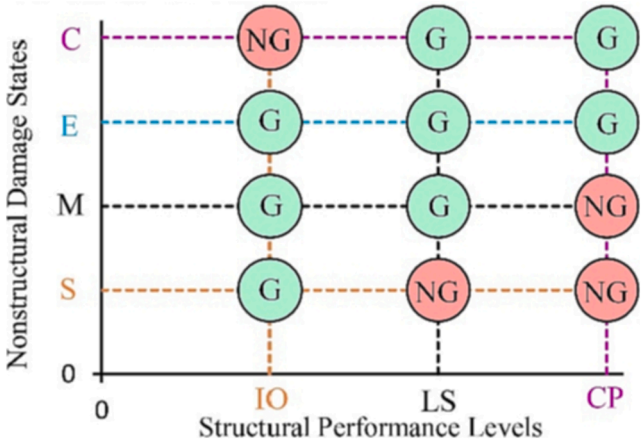

Fig. 7. Considered overall performance levels of a structure, on the basis of the performance levels of the structural components and the damage levels of the non-structural ones.

The performance levels of Immediate Occupancy (IO), Life Safety (LS), and Collapse Prevention (CP) have been allowed for in the analysis, with the corresponding inter-story drift values equal to 0.7, 2.5, and 5 %

Table 3
Reliability (values given as percentages) of (left) structural and (right) non-structural members, under different earthquake intensity levels: (top) frequent earthquake, FE; (middle) design basis earthquake, DBE; (bottom) maximum considered earthquake, MCE.

FE	Structural components			Non-Structural components			
	IO	LS	CP	S	M	E	C
5-Storey	99.99	100	100	99.70	100	100	100
10-Storey	99.99	100	100	99.77	100	100	100
15-Storey	99.99	100	100	99.99	100	100	100
DBE	Structural components			Non-Structural components			
	IO	LS	CP	S	M	E	C
5-Storey	0.00	99.99	100	0.00	0.85	99.25	100
10-Storey	0.00	97.13	100	0.00	0.00	99.96	100
15-Storey	0.00	85.86	100	0.00	0.00	99.95	100
MCE	Structural components			Non-structural components			
	IO	LS	CP	S	M	E	C
5-Storey	0.00	83.26	100	0.00	0.00	88.52	100
10-Storey	0.00	28.07	99.45	0.00	0.00	68.16	100
15-Storey	0.00	17.58	99.91	0.00	0.00	39.88	99.99

[37]. The slight, moderate, extensive, and complete damage levels have been instead adopted for the non-structural components, with the corresponding acceleration values respectively given by 0.25 g, 0.5 g, 1 g, and 2 g [38]. Since this study aims at proposing a new method for seismic reliability analysis and comparing it with standard procedures, the aforementioned limit states could be replaced or even complemented by others.

For each target earthquake, the performance of the entire structure is deemed appropriate when there is consistency between the damage levels of its structural and non-structural components. For a frequent earthquake, it is expected that the structural components do not experience a significant strength or stiffness loss, so that the system remains serviceable (IO). On the other hand, the LS and CP performance levels are respectively targeted for the design basis and the maximum considered earthquakes. The sketch provided in Fig. 7 in matrix form, with the performance levels for the structural components along the horizontal axis and the damage states for the non-structural components along the vertical axis, allows distinguishing the allowable pairs (flagged as G, or good) and those not allowed for in the analysis, being considered inconsistent (flagged as NG, or no-good).

According to the results depicted in Fig. 6, the reliability under each hazard level has been computed for all the performance and damage levels. The relevant outcomes are collected in Table 3. Results indicate that for some cases, for instance, the IO performance level of structural components or the slight damage of non-structural components under both DBE or MCE hazard levels, zero reliability values are obtained; hence, under such hazard levels, these damages will be surely experienced. The other way around, under the FE hazard level a high reliability is expected and indeed obtained even for low damage levels: for instance, the reliability of both structural and non-structural components exceeds 99.5 %. Hence, the non-structural components do not have a significant influence on the reliability of the structures for this earthquake intensity.

It is worth noting that the reliability of non-structural components under the DBE and MCE earthquakes is shown to be smaller than that of the structural elements. The mentioned issue is especially evident for the lower damage levels in the non-structural elements. Looking at the results corresponding to the DBE and considering the LS performance level for the structural elements and the moderate damage level for non-structural elements, the difference between the reliability values turned out to exceed 85 %, being 99.14 %, 97.13 %, and 85.86 % for the 5-, 10- and 15-story structures respectively. Looking instead at the results corresponding to the MCE and considering the CP performance

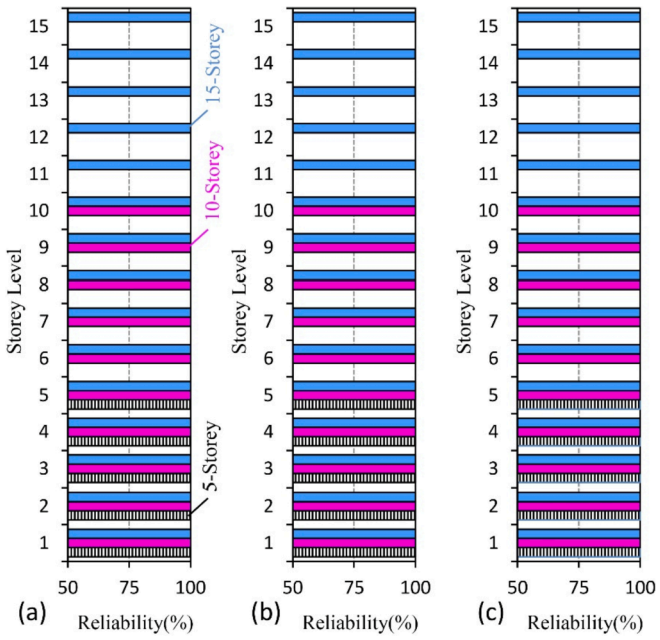

Fig. 8. Frequent earthquake, story-wise reliability corresponding to: (a) IO performance level for the structural components; (b) Slight damage level for the non-structural components; (c) Moderate damage level for the non-structural components.

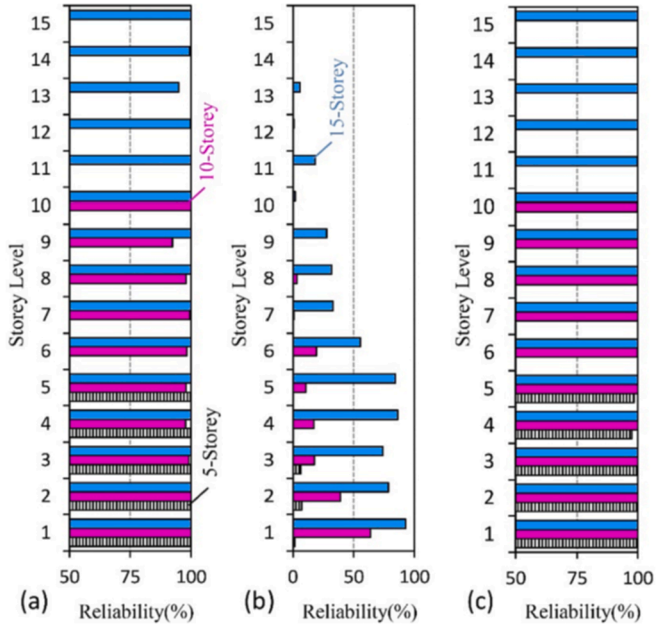

Fig. 9. Design basis earthquake, story-wise reliability corresponding to: (a) LS performance level for the structural components; (b) Moderate damage level for the non-structural components; (c) Extensive damage level for the non-structural components.

level for the structural components and the extensive damage level for non-structural elements, the difference in the reliability values varies between 11.48 % for the 5-story structure and 60.03 % for the 15-story-one. Such huge differences in the reliability values clearly show the importance of the non-structural members when the seismic reliability of the entire building has to be evaluated.

The methodology described so far is rather standard, and brings some shortcomings. The main one is the recording of the maximum values of the inter-story drifts and of the lateral accelerations to

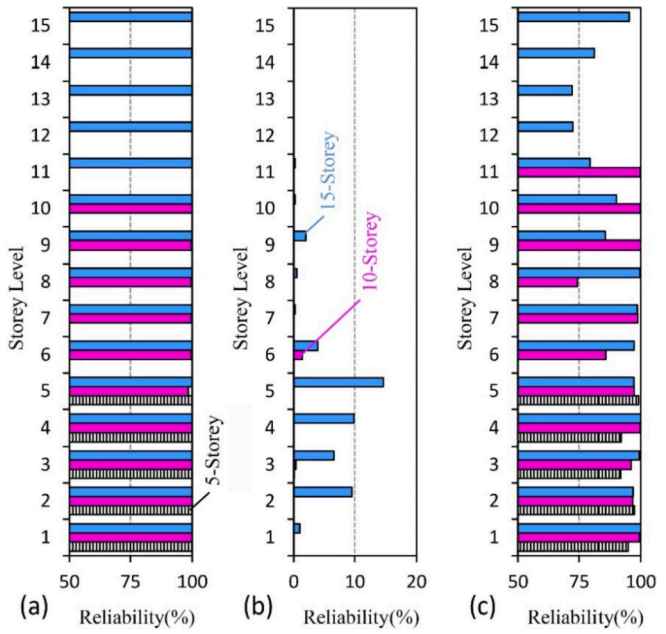

Fig. 10. Maximum considered earthquake, story-wise reliability corresponding to: (a) CP performance level for the structural components; (b) Moderate damage level for the non-structural components; (c) Extensive damage level for the non-structural components.

Table 4
Comparison between the reliability indices of (left) structural and (right) non-structural members provided by the conventional approach (method 1) and by the story-wise approach (method 2), under different earthquake intensity levels: (top) frequent earthquake, FE; (middle) design basis earthquake, DBE; (bottom) maximum considered earthquake, MCE.

FE	Structural components		Non-Structural components			
	Method 1	Method 2	Method 1		Method 2	
	IO	IO	S	M	S	M
5-Storey	99.99	99.9	99.70	100	99.73	100
10-Storey	99.99	100	99.77	100	99.99	100
15-Storey	99.99	100	99.99	100	99.97	100
DBE	**Structural components**		**Non-Structural components**			
	Method 1	Method 2	Method 1		Method 2	
	LS	LS	M	E	M	E
5-Storey	99.99	99.99	0.85	99.25	0.22	97.41
10-Storey	97.13	92.40	0.00	99.96	0.00	99.81
15-Storey	85.86	95.02	0.00	99.95	0.00	99.77
MCE	**Structural components**		**Non-Structural components**			
	Method 1	Method 2	Method 1		Method 2	
	CP	CP	E	C	E	C
5-Storey	100	99.99	88.52	100	91.73	100
10-Storey	99.45	98.51	68.16	100	74.40	100
15-Storey	99.91	99.87	39.88	99.99	72.14	100

characterize the structural response to the ground motion, regardless of the corresponding localizations along the vertical axis of the structure. Accordingly, the location of maximum damage induced by the earthquake is not provided as an output of this approach. Since different ground motions may result in different damage patterns, the way the whole building reliability is affected by the damage levels at different stories cannot be determined by this approach. A methodology to account for these effects too is therefore proposed next.

4.2. Story-wise reliability analysis

A way to solve the above-mentioned issue linked to the incapability of the standard procedure to deal with different damage patterns induced by the ground motions is to perform a separate reliability analysis for each story. To this purpose, for each intensity level and at each story of the building, the values of the maximum drift and the absolute acceleration have been recorded during the analysis. Next, the reliabilities of structural and non-structural components have been computed separately, following the same procedure described in Section 0.1.

The resulting story-wise solutions are reported in Figs. 8–10 for the three considered structural frames. This representation allows showing the reliability values of each story and, accordingly, the critical location of the damage for each structure. While in agreement with the former results, the current ones grant a deeper assessment of the interaction between the structural and non-structural components.

It can be observed that the results achieved with the conventional method are close to the minimum values obtained with the present method, see Table 4. In this table, it is shown that under the FE the reliability indices of both structural and non-structural components are still larger than 99.5 %. Under higher seismic intensities, the indices relevant to the non-structural components are always considerably smaller than those related to the structural ones. Regarding the DBE, by allowing for the LS performance level of the structural components and the M damage level of the non-structural elements, the difference between the indices computed for the two groups amounts to 92.4 %, at least. Regarding the MCE, by considering the CP performance level of the structural components and the E damage level of the non-structural elements, the same difference between the two indices varies in the range of 8.26–27.73 %, with a higher value for the taller building.

By getting more into the details of the results reported in Figs. 8–10, the non-structural elements of the higher stories display lower reliability and, if sufficient support is not provided, their falling may cause accidents and casualties. This result highlights the importance of proper design and construction of the non-structural components, which have therefore to be included in any seismic reliability analysis at the building level.

4.3. Seismic reliability analysis using a block diagram approach (combined method)

The reliabilities of structural and non-structural components have been so far determined independently but, since the performance of the system is defined by the performance of all of its components, it might look inappropriate to perform two different and separate reliability analyses.

Under an assigned seismic action, if structural and non-structural elements of a story or, on a larger scale, of the entire building are distinguished into different groups, the probability that a certain performance level is exceeded can be determined for each group independently, via the conventional methods already discussed. When the combined reliability related to different damage levels in the structural elements is instead considered, such methods are not applicable anymore. In complex systems with groups of elements having different functions and being characterized by means of different limit states, the mentioned weakness of the former methods in determining the overall reliability of the system becomes clear, see [33].

To address this issue, a Reliability Block Diagram (RBD) method is here proposed, see also [39,40]. In the following, this methodology is first described and then adopted to assess the reliability of the structures under two different scenarios, by either considering or not the non-structural components.

The RBD method is based on a representation of the physical arrangement of system components: the system is first broken down into subsystems, with a block used to describe each of them. Blocks can be

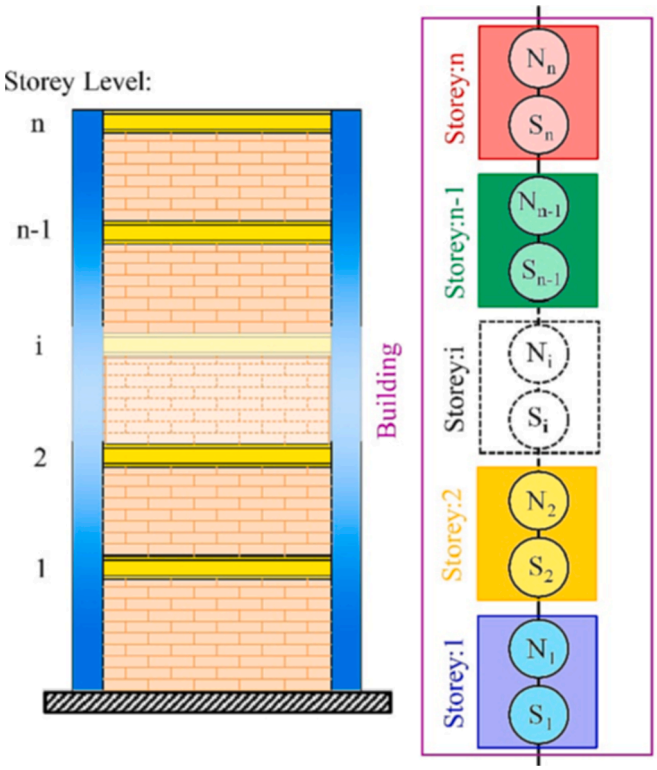

Fig. 11. Sketch of the considered configuration for the *n*-story structure.

stacked in series, parallel, or in more complex ways to account for the way the components work to define the service conditions of the system. Having defined the block diagram, the overall reliability indices for the system can be estimated [41] by means of appropriate techniques to quantify the reliability of each block.

By considering a series system consisting of n subsystems (primarily given by the number of stories), the whole system itself is assumed to serve as long as each component does. If R_i, with $i = 1, \cdots, n$, is the reliability of i^{th} component, and if the strengths of the components are assumed independent of each other, the reliability R of the whole system is given by:

$$R = R_1 \bullet R_2 \cdots R_{(n-1)} \bullet R_n = \prod_{i=1}^{n} R_i \leq \min\{R_i\} \tag{5}$$

which shows that R itself cannot be larger than the smallest reliability value, see also [42]. By assuming that the failure of one story only, makes the structure not serviceable anymore, the structure itself can be assumed as a system consisting of n series components, as sketched in Fig. 11. Assuming that each story is serviceable provided that both the structural (S) and the non-structural (N) components are serviceable on their own and at the same time, each story can be modeled as a series system consisting of these two sub-components. This assumption stems from the fact that the structure is not serviceable anymore even in the case of complete damage of non-structural components only; for instance, as depicted in Fig. 1, this may happen when the structural system is not critically damaged. For the configuration shown in Fig. 11, the whole reliability can be thus computed as:

$$R = \prod_{i=1}^{n} R_i(S) \bullet R_i(N) \tag{6}$$

where $R_i(S)$ and $R_i(N)$ are, respectively, the reliability indices related to the structural and non-structural components.

A summary of the hierarchy in the computation of the reliability for structures with a configuration as depicted in Fig. 11, is as follows:

i. Under the considered hazard level, the reliability curve is determined for the structural and non-structural components of each story.
ii. The reliability curves of the structural and non-structural components are combined to obtain the reliability curve of each story and for each damage state, see Fig. 12.
iii. The reliability curves of the stories are finally combined to define the reliability curve of the whole structure, for each performance and damage level in the structural and non-structural components, and for each considered hazard level, see Fig. 13.

This methodology has led to the reliability curves shown in Figs. 14–16 for the three considered structural frames, under the effects of the FE, DBE, and MCE earthquakes, respectively. As before, different combinations of performance and damage levels in structural and non-structural components are reported. Under the FE, for the different

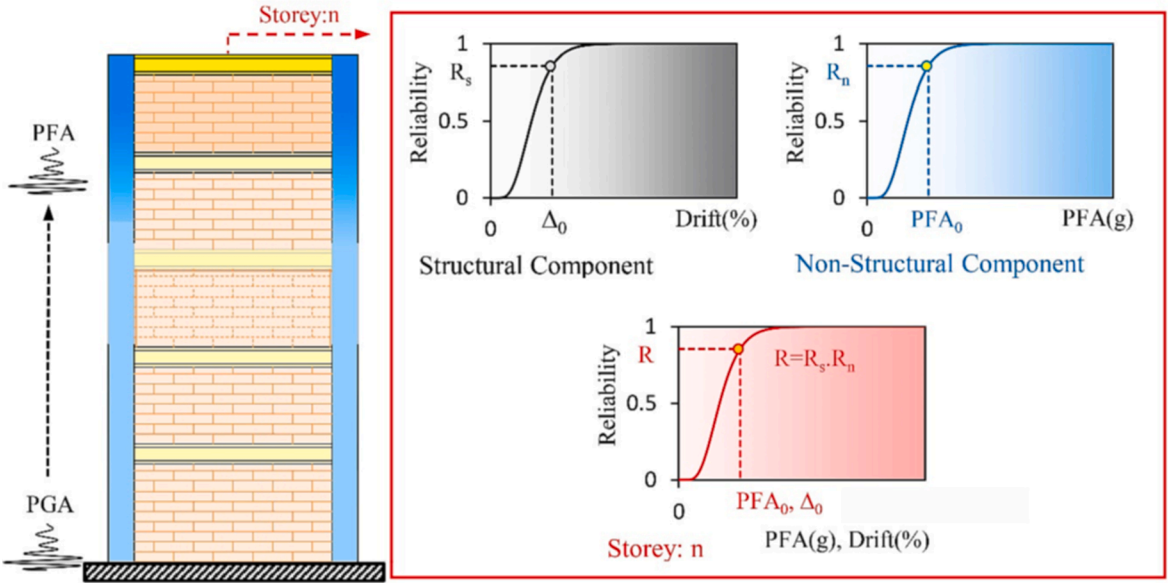

Fig. 12. Schematic of the definition of the reliability curve for a single story.

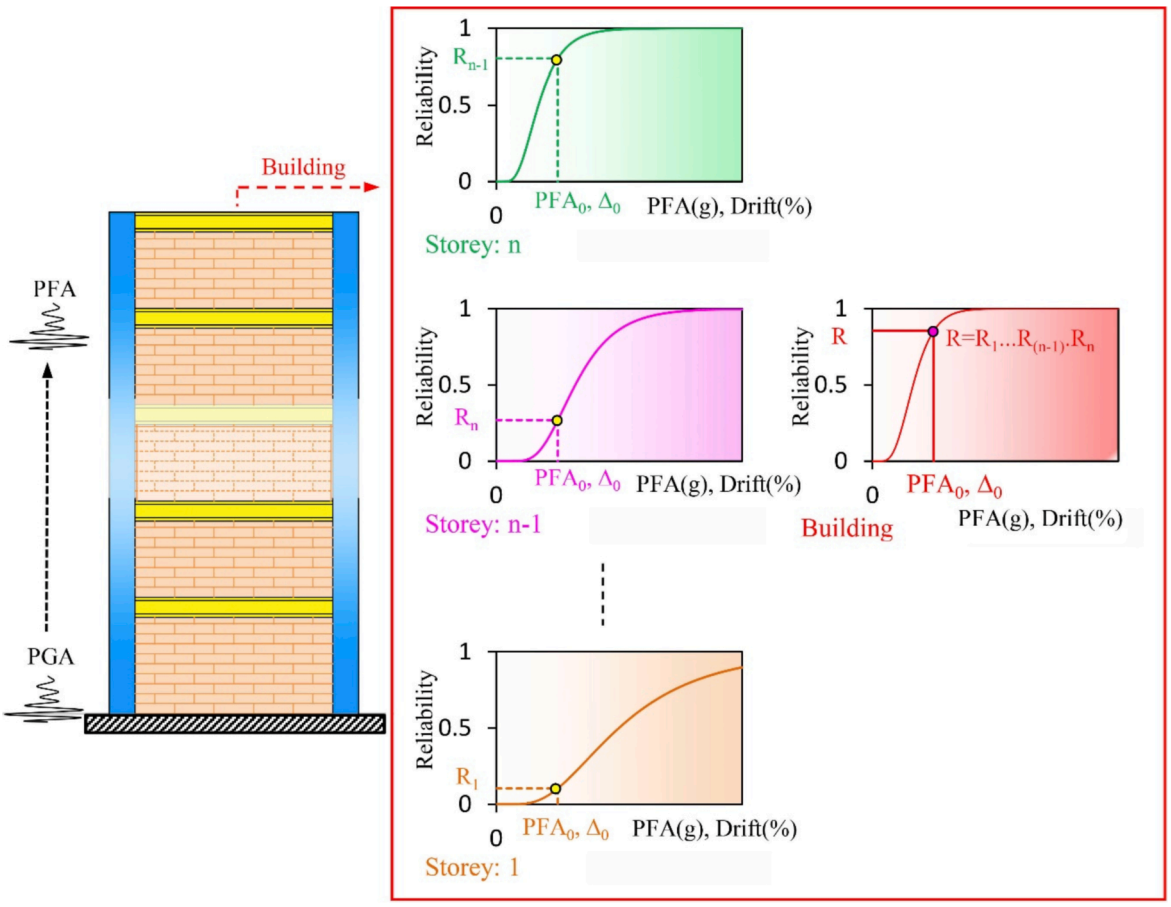

Fig. 13. Schematic of the definition of the reliability curve for the whole structure.

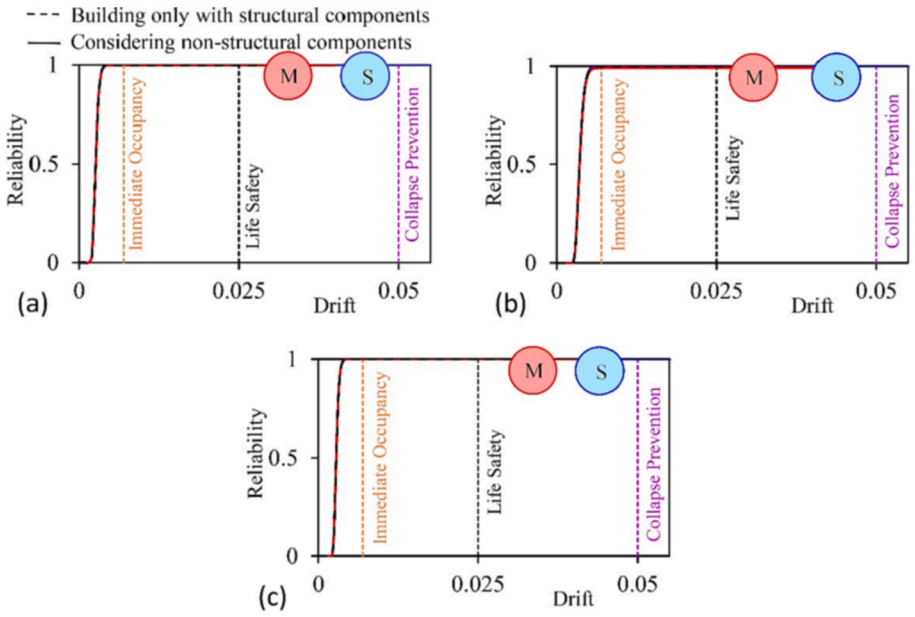

Fig. 14. Frequent ground motion, seismic reliability curves obtained by either considering or ignoring the effects of the non-structural components: (a) 5-, (b) 10- and (c) 15-story buildings.

damage levels related to the non-structural components, the overall reliability of the structure is always estimated as 100 %. In accordance with the results of the previous sections, for this intensity level, the non-structural components do not affect the reliability of the entire structure. The other way around, under the DBE and the MCE the role of the non-structural components in reducing the overall reliability of the structures is instead shown to be quite significant. Specifically, under the DBE and by considering the LS performance level for the structural

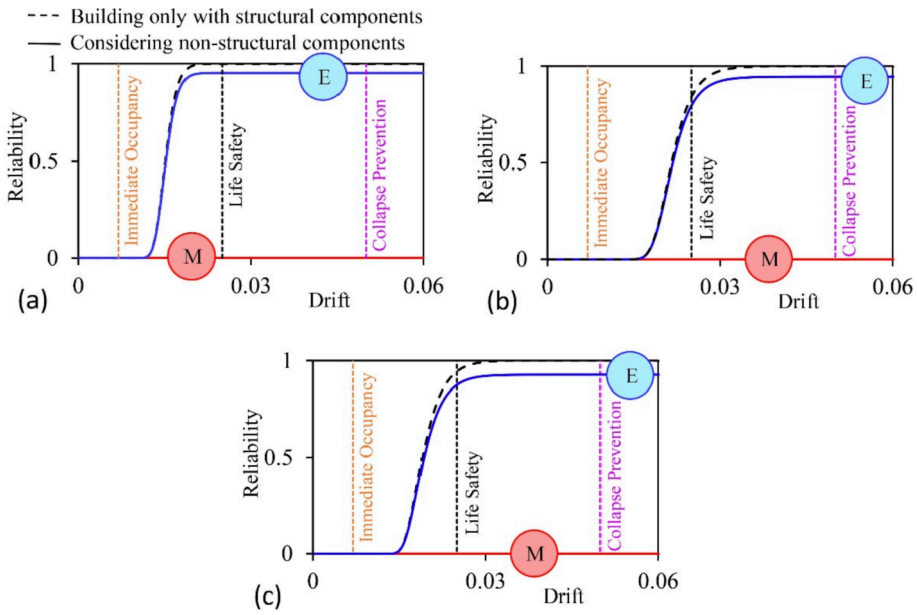

Fig. 15. Design basis ground motion, comparison between the seismic reliability curves obtained by either considering or ignoring the effects of the non-structural components: (a) 5-, (b) 10- and (c) 15-story buildings.

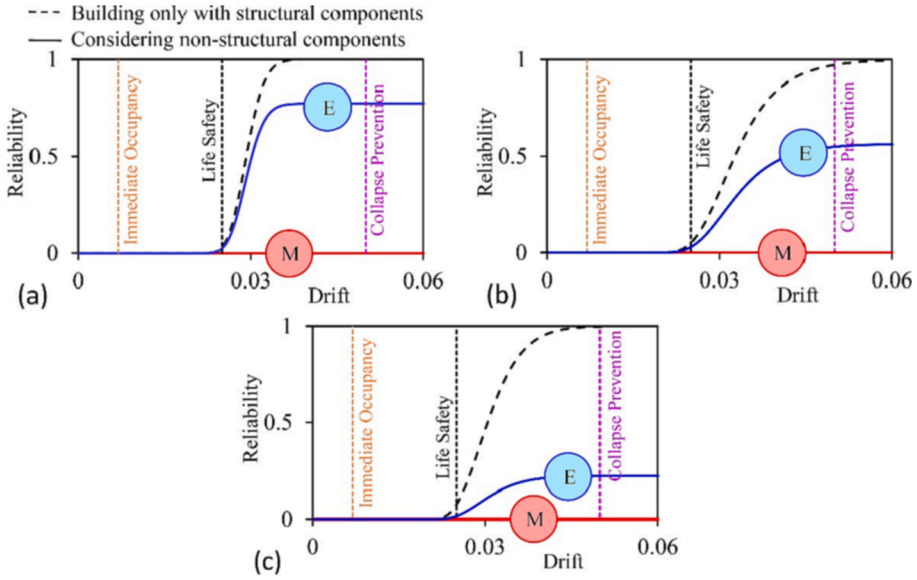

Fig. 16. Maximum considered ground motion, comparison between the seismic reliability curves obtained by either considering or ignoring the effects of the non-structural components: (a) 5-, (b) 10- and (c) 15-story buildings.

components and the M damage level for the non-structural components, the latter reduce the overall reliability by 99.99 %, 84.05 %, and 94.4 % for 5-, 10- and 15-story structures, respectively. Under the MCE and by taking into account the CP performance level for the structural components and the E damage for the non-structural components, the overall reliability is instead reduced by 22.63 %, 42.24 %, and 77.88 % for 5-, 10- and 15-story buildings, respectively.

By comparing the reliability curves reported in these figures and obtained by allowing or not for the effects of the non-structural components, the important role of these last elements is clearly highlighted in the definition of the seismic reliability of the entire structure under higher earthquake intensity levels.

4.4. Combined reliability analysis of the structure using the performance areas approach

Besides the limit states considered in what precedes, others characterized by different damage levels can be accounted for in the analysis, since in reality damage is a parameter taking values in a continuous range, e.g. [01) if assumed to scale the stiffness of the elements. To set the seismic performance of systems, it is often sufficient to provide results for certain damage levels, while all the other possible states in between are not considered. To cover these additional damage states in seismic reliability analysis, it is necessary to define performance areas and provide the relevant reliability values for them. By defining a range of values for each damage state, the probability intervals can be computed and the relevant mean value can be adopted as a criterion to characterize each range. Fig. 17(a) provides a clear picture of this

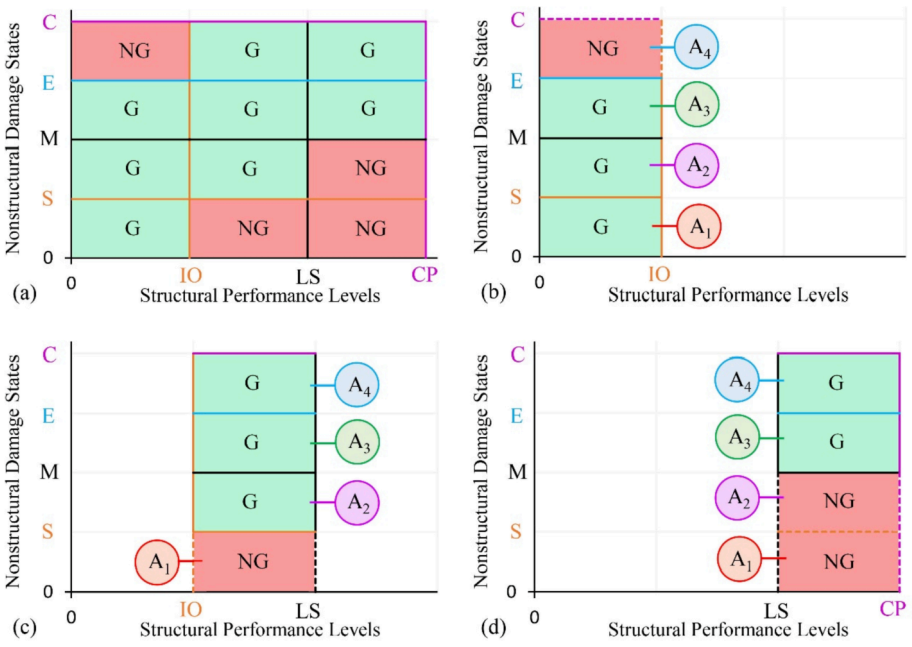

Fig. 17. Combined performance levels for structural and non-structural components: (a) overall view of the considered desirable performance areas, A_i, for different hazard levels, (b) Performance areas for FE hazard level, (c) Performance areas for MCE hazard level, (d) Performance areas for DBE hazard level.

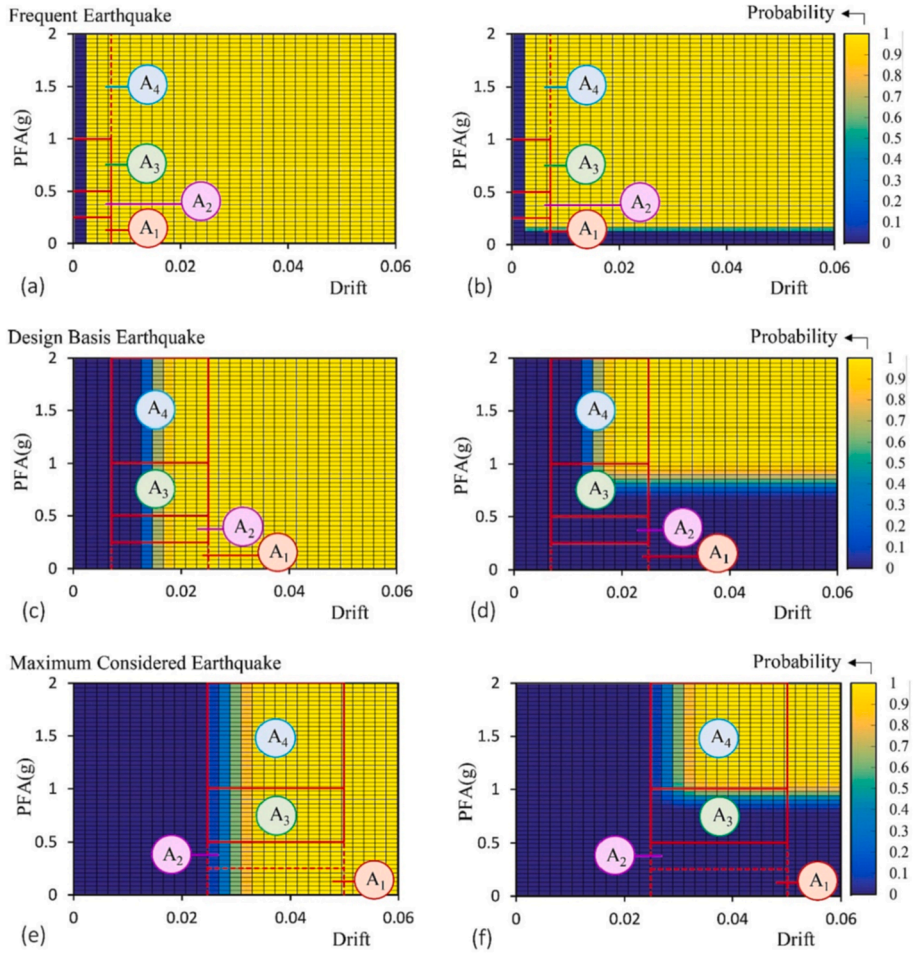

Fig. 18. Reliability levels of the 5-story structure, under: FE (a and b), DBE (c and d), and MCE (e and f). Results obtained by considering the structural components only (a, c and e), or both the structural and non-structural components (b, d and f).

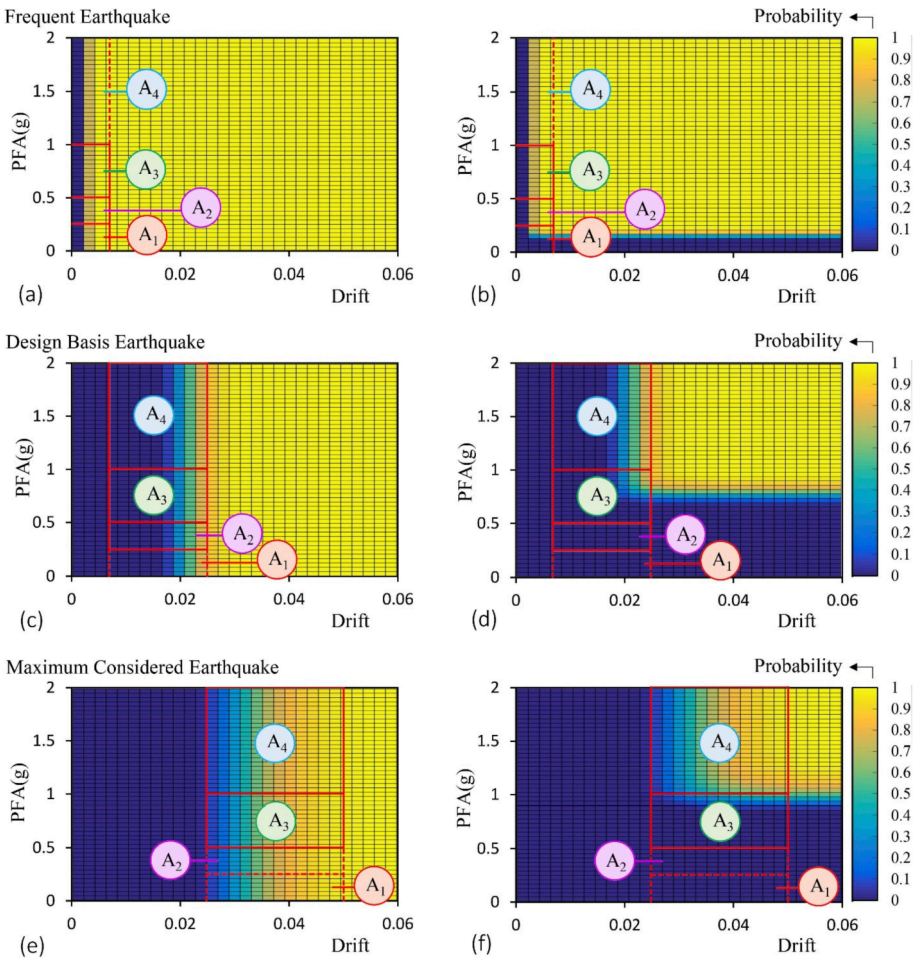

Fig. 19. Reliability levels of the 10-story structure, under: FE (a and b), DBE (c and d), and MCE (e and f). Results obtained by considering the structural components only (a, c and e), or both the structural and non-structural components (b, d and f).

approach based on the performance areas, and represents a generalization of what is reported in Fig. 7 for some characteristic values only of the performance values and damage states. In the performance-based evaluation, the goal is to check whether under a certain seismic intensity, the desired performance level is achieved or not. Therefore, it is required that the A_i areas are selected corresponding to the target hazard level. It is expected that the structural components experience IO, LS, and CP performance levels under FE, DBE, and MCE hazard levels, respectively. Accordingly, in this study, the desired performance areas for each hazard level are selected as depicted in Fig. 17b–d.

By exploiting the combined approach of Section 3.3, the reliability analysis has been performed on the considered structures by either allowing for the effects of the non-structural components or not. The results are reported in Figs. 18–20, respectively for the 5-, 10- and 15-story structures. To keep consistency with the performance and damage levels considered before, the definition of the boundary states is again as shown in Fig. 7. In these plots the areas characterized by inconsistent performance levels, in terms of damage states of the structural and non-structural components, are highlighted by means of dashed lines along their boundaries, see e.g. area A_4 under the FE hazard level. The value provided in the contour plots represents the probability of not attaining specific values of drift and PFA: while in the literature a single number stands as the reliability related to a given limit state, with the proposed approach it is possible to account that damage is a continuous parameter, and a spectrum of limit states can be allowed for (see e.g. Fig. 20). The charts thus consist of a large number of reliability curves.

With this approach, the maximum story drift considered for the FE has been up to 0.7 %, while for the DBE and the MCE the allowable ranges have been set between 0.7 % and 2.5 %, and between 2.5 and 5 %, respectively. Additional details related to these values and a thorough discussion can be found in [37,38].

These results are summarized in Table 5. Here it emerges that, by allowing for the non-structural components, the reliability of the structures is reduced considerably, as shown also by the yellow areas in the graphs. The rate of the mentioned reduction obviously varies depending on the magnitude of the earthquake: for high levels of damage allowed in the non-structural components, the impact on the results is accordingly decreased.

Under the FE, for the optimal combination of performance levels of the structural and non-structural components leading to the overall performance level A_1, the reduction amounts to 40.26 %, 32.9 %, and 31.98 % for 5-, 10- and 15-story structures, respectively. The decrease in the reliability index with the structural height can be attributed to the increased values of story drift and acceleration for taller structures; even if story drifts are limited, the story acceleration increases from the bottom to the top stories, see [11]. According to Figs. 8–10, also the reliability of the non-structural components in several stories of taller buildings will be lower.

For the DBE, the two zones A_2 and A_3 are considered as the optimally combined performance levels. Compared to when only the structural components are considered in the reliability analysis process, and for all of the studied structures, the reliability in area A_2 is reduced to zero. This represents a definite violation of the desired combined performance levels: LS for structural components and M for non-structural components. For performance level A_3, the reduction varies instead from 36.21

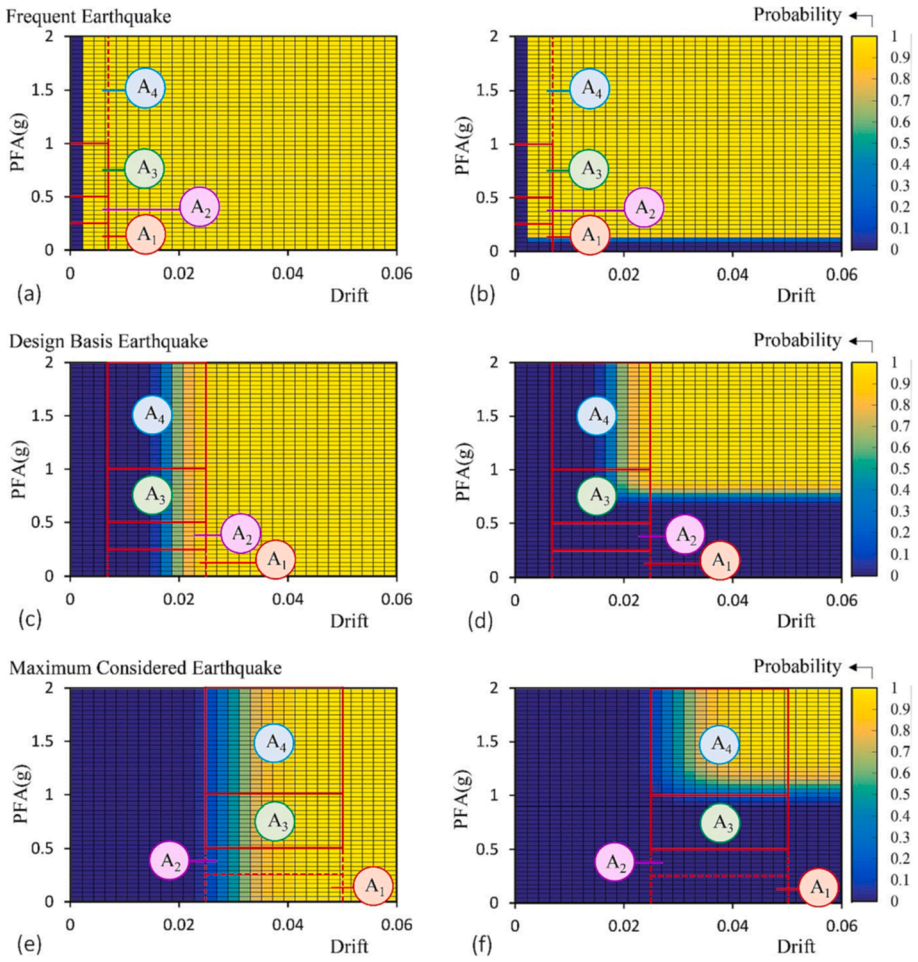

Fig. 20. Reliability levels of the 15-story structure, under: FE (a and b), DBE (c and d), and MCE (e and f). Results obtained by considering the structural components only (a, c and e), or both the structural and non-structural components (b, d and f).

Table 5
Mean values of the reliability indices of (condition a) structural and (condition b) both structural and non-structural members, under the frequent earthquake, FE, the design basis earthquake, DBE and the maximum considered earthquake, MCE intensity levels.

5-Storey	FE		DBE		MCE	
	Structural components	Structural and Non-Structural components	Structural components	Structural and Non-Structural components	Structural components	Structural and Non-Structural components
A_1	63.12	22.86	54.70	0.00	83.43	0.00
A_2	63.12	63.11	54.70	0.00	83.43	0.00
A_3	63.12	63.11	54.70	18.49	83.43	12.21
A_4	63.12	63.11	54.70	54.58	83.43	82.43
10-Storey	FE		DBE		MCE	
	Structural components	Structural and Non-Structural components	Structural components	Structural and Non-Structural components	Structural components	Structural and Non-Structural components
A_1	48.59	15.68	19.69	0.00	98.42	0.00
A_2	48.59	48.56	19.69	0.00	98.42	0.00
A_3	48.59	48.56	19.69	8.46	98.42	5.14
A_4	48.59	48.56	19.69	19.68	98.42	63.52
15-Storey	FE		DBE		MCE	
	Structural components	Structural and Non-Structural components	Structural components	Structural and Non-Structural components	Structural components	Structural and Non-Structural components
A_1	60.21	28.23	31.76	0.00	76.16	0.00
A_2	60.21	60.20	31.76	0.00	76.16	0.00
A_3	60.21	60.20	31.76	14.39	76.16	1.67
A_4	60.21	60.20	31.76	31.75	76.16	69.21

% for the 5-story structure to 11.23 % and 17.37 % for the 10- and 15-story structures, respectively.

Under the MCE, by considering the performance areas A_3 and A_4 as the acceptable ones, the reduction trend is significant. In the performance area A_3, a reduction of more than 70 % is estimated (71.22 %, 93.28 % and 74.49 % for the 5-, 10- and 15-story buildings, respectively). The reduction in the performance area A_4 is instead estimated as 1 % for the 5-story structure, 34.9 % for the 10-story structure, and 6.95 % for 15-story structure.

5. Discussion and conclusion

To study the reliability of multi-story steel frames under the action of ground motions, in this paper the effects of the non-structural components have been accounted for. By defining consistent levels of damage allowed for by the limit states relevant to the structural members on one side, and to the non-structural components on the other, the seismic behavior of structures has been assessed with three different methods: a conventional one, dealing with structural and non-structural components separately at the entire structural level; a more refined one, still handling the structural and non-structural components separately, but at the story level; a newly proposed hierarchical one, resting on the results of the previous method but adopting a combination in series of structural and non-structural parts at the story level, and then a further combination in series of all the stories to define the reliability of the entire building. For each approach, the relevant strengths and weaknesses have been discussed.

The probabilistic distributions of the maximum drift and the absolute story acceleration, respectively used as characteristic response features of structural and non-structural components, have been obtained under the three hazard levels corresponding to the frequent, design basis, and the maximum considered earthquakes. The results obtained with the three methods are shown to be consistent with each other and showcased the importance of the non-structural components in setting the reliability, or performance level of the entire structure. By accounting for the specific features of the newly proposed block diagram-based method, and for its ability to circumvent the weaknesses of the other two methods, its use in seismic reliability analysis is recommended. To cope with damage states additional to those related to the customarily adopted limit states, the idea of performance areas has been also put forward and exploited. Based on the presented results using different methods, the following conclusions can be drawn:

1. Under the frequent earthquake, by considering the IO level for the structural components and the slight damage level for non-structural ones, the reliability indices are obtained as large as 99.5 %.
2. Under the design basis earthquake, by considering the LS performance level for the structural components and the moderate damage level for the non-structural ones, the latter reduces the overall reliability of the structures by at least 84 % in comparison with the analysis allowing for the structural components only.
3. Under the maximum considered earthquake, by considering the CP performance level for the structural components and the extensive damage for the non-structural ones, the non-structural components reduce the overall reliability of structures by values in the range 22–78 %, depending on the number of stories, if compared with the analysis disregarding the said non-structural components.

It should be noted that the above conclusions are limited to the adopted assumptions, analyzed structures, and utilized ground motion records. To ease the understanding of the proposed methodology, in the present study only a simple lateral load-carrying structural system and acceleration-sensitive non-structural components have been considered. Obviously, the structural system (single, dual, or multilevel), the adopted approach to reliability analysis (constant hazard or constant damage level) [29], and the type of the non-structural components (displacement-sensitive, acceleration-sensitive or simultaneously sensitive to displacements and accelerations) can affect the way the equivalent block diagram of the entire structure is built. In future works, the proposed methodology will be therefore extended to deal with these additional factors.

CRediT authorship contribution statement

Vahid Mohsenian: Conceptualization, Methodology, Formal analysis, Investigation, Visualization. **Nima Gharaei-Moghaddam:** Investigation, Resources, Writing – original draft. **Stefano Mariani:** Supervision, Validation, Writing – review & editing. **Iman Hajirasouliha:** Validation, Writing – review & editing, Supervision.

Declaration of Competing Interest

The authors declare that they have no known competing financial interests or personal relationships that could have appeared to influence the work reported in this paper.

References

[1] Fierro EA, Reitherman R. Reducing the risks of nonstructural earthquake damage: a practical guide. DIANE Publishing; 1995.
[2] Farsangi, Ehsan Noroozinejad, et al., Reliability-based analysis and design of structures and infrastructure. 2021: CRC Press.
[3] Farsangi EN, et al. Resilient structures and infrastructure. Springer; 2019.
[4] Zhou H, et al. Reproducing response spectra in shaking table tests of nonstructural components. Soil Dyn Earthq Eng 2019;127:105835.
[5] Jenkins C, et al. Experimental fragility analysis of cold-formed steel-framed partition wall systems. Thin-Walled Struct 2016;103:115–27.
[6] Hou H, et al. Horizontal seismic force demands on nonstructural components in low-rise steel building frames with tension-only braces. Eng Struct 2018;168:852–64.
[7] Raffaele L, et al. Seismic response assessment of architectural non-structural LWS drywall components through experimental tests. J Constr Steel Res 2019;162:105575.
[8] Anajafi H, Medina RA. Evaluation of ASCE 7 equations for designing acceleration-sensitive nonstructural components using data from instrumented buildings. Earthq Eng Struct Dyn 2018;47(4):1075–94.
[9] Magliulo G, Petrone C, Manfredi G, Demand S. on Acceleration-Sensitive Nonstructural Components. In: Papadrakakis M, Plevris V, Lagaros ND, editors. Computational Methods in Earthquake Engineering, Volume 3. Cham: Springer International Publishing; 2017. p. 177–204.
[10] Fathali S, Lizundia B. Evaluation of current seismic design equations for nonstructural components in tall buildings using strong motion records. Struct Design Tall Spec Build 2011;20(S1):30–46.
[11] Mohsenian V, Gharaei-Moghaddam N, Hajirasouliha I. Multilevel seismic demand prediction for acceleration-sensitive non-structural components. Eng Struct 2019;200:109713.
[12] Salari N, et al. Demands on acceleration-sensitive nonstructural components in special concentrically braced frame and special moment frame buildings. Eng Struct 2022;260:114031.
[13] Lima C, Martinelli E. Seismic response of acceleration-sensitive non-structural components in buildings. Buildings 2019;9(1):7.
[14] Villaverde R. Simple method to estimate the seismic nonlinear response of nonstructural components in buildings. Eng Struct 2006;28(8):1209–21.
[15] Wang T, Shang Q, Li J. Seismic force demands on acceleration-sensitive nonstructural components: A state-of-the-art review. Earthq Eng Eng Vib 2021;20(1):39–62.
[16] Sullivan TJ. Post-earthquake reparability of buildings: The role of non-structural elements. Struct Eng Int 2020;30(2):217–23.
[17] Perrone D, et al. A framework for the quantification of non-structural seismic performance factors. J Earthq Eng 2022:1–27.
[18] Mahsuli M, Haukaas T. Seismic risk analysis with reliability methods, part II: Analysis. Struct Saf 2013;42:63–74.
[19] Kuo K-C, et al. Evaluation of nonstructural component fragilities in risk assessment of hospitals. in *4th International Conference on Earthquake Engineering, Paper*. Citeseer; 2006.
[20] Cremen G, Baker JW. Improving FEMA P-58 non-structural component fragility functions and loss predictions. Bull Earthq Eng 2019;17(4):1941–60.
[21] ASTM, *A36M-19, Standard Specification for Carbon Structural Steel*. 2019, ASTM International: West Conshohocken.
[22] Aisc. ANSI/AISC 360–10, Specification for structural steel buildings. USA: American Institute of Steel Construction Chicago-Illinois; 2010.
[23] CSI, *ETABS, Extended Three Dimensional Analysis of Building Systems Nonlinear*, in *Structural and Earthquake Engineering Software*. 2015, Computers and Structures Inc.: Berkeley, CA, USA.

[24] ASCE, ASCE, SEI 7–10, Minimum design loads and associated criteria for buildings and other structures. American Society of Civil Engineers: Reston 2010 Virginia USA.
[25] CSI, *PERFORM-3D Nonlinear Analysis and Performance Assessment for 3D Structures*, in *Structural and Earthquake Engineering Software*. 2017, Computers and Structures Inc.: Berkeley, CA, USA.
[26] Asce, asce, sei,. 41–17: seismic evaluation and retrofit of existing buildings. American Society of Civil Engineers; 2017.
[27] Taghavi S, Miranda E. Probabilistic seismic assessment of floor acceleration demands in multi-story buildings. John A Blume Earthquake Eng Center 2006.
[28] Taghavi-Ardakan S. Probabilistic seismic assessment of floor acceleration demands in multi-story buildings. Stanford University; 2006.
[29] Singh AK, Ang A-H-S. Stochastic prediction of maximum seismic response of light secondary systems. Nucl Eng Des 1974;29(2):218–30.
[30] 2800, Permanent Committee for Revising the Standard, *Iranian Code of Practice for Seismic Resistant Design of Buildings*. 2014, Building and Housing Research Cente: Tehran, Iran.
[31] Hancock J, et al. An improved method of matching response spectra of recorded earthquake ground motion using wavelets. J Earthq Eng 2006;10(spec01):67–89.
[32] PEER, *PEER Ground Motion Database*. Pacific Earthquake Engineering Research Center.
[33] Mohsenian V, Hajirasouliha I, Filizadeh R. Seismic reliability analysis of steel moment-resisting frames retrofitted by vertical link elements using combined series–parallel system approach. Bull Earthq Eng 2021;19(2):831–62.
[34] Mohsenian V, Gharaei-Moghaddam N, Arabshahi A. Evaluation of the probabilistic distribution of statistical data used in the process of developing fragility curves. Int J Steel Struct 2022;22(4):1002–24.
[35] Mohsenian, Vahid, Iman Hajirasouliha, and Reza Filizadeh, *Seismic reliability assessment of steel moment-resisting frames using Bayes estimators*. Proceedings of the Institution of Civil Engineers-Structures and Buildings, 2021: p. 1-15.
[36] Zareian F, et al. *Basic concepts and performance measures in prediction of collapse of buildings under earthquake ground motions*. The. Struct Des Tall Special Build 2010; 19(1–2):167–81.
[37] Asce, asce, sei41-13,. Seismic rehabilitation of existing buildings. American Society of Civil Engineers; 2014.
[38] RMS, *Earthquake Loss Estimation Method-HAZUS97 Technical Manual*. 1997, National Institute of Building Sciences: Washington D.C., USA.
[39] Mohsenian V, Gharaei-Moghaddam N, Hajirasouliha I. Reliability analysis and multi-level response modification factors for buckling restrained braced frames. J Constr Steel Res 2020;171:106137.
[40] Mohsenian V, et al. Seismic reliability assessment of RC tunnel-form structures with geometric irregularities using a combined system approach. Soil Dyn Earthq Eng 2020;139:106356.
[41] Mortezaei A, Mohsenian V. Reliability-based seismic assessment of multi-story box system buildings under the accidental torsion. J Earthq Eng 2022;26(2):674–97.
[42] Nowak, Andrzej S and Kevin R Collins, *Reliability of structures*. 2012: CRC press.